Medical Engineering and Physics 69 (2019) 50–57

Contents lists available at ScienceDirect

Medical Engineering and Physics

journal homepage: www.elsevier.com/locate/medengphy

sEMG-signal and IMU sensor-based gait sub-phase detection and prediction using a user-adaptive classifier

Jaehwan Ryu, Byeong-Hyeon Lee, Junho Maeng, Deok-Hwan Kim*

Department of Electronic Engineering, Inha University, Incheon 402-751, South Korea

ARTICLE INFO

Article history:
Received 14 June 2018
Revised 17 April 2019
Accepted 19 May 2019

Keywords:
Electromyogram
Gait sub-phase detection
Gait cycle
Gait prediction
Lower-limb power-assist robot

ABSTRACT

This paper presents a gait sub-phase detection and prediction approach using surface electromyogram (sEMG) signals, pressure sensors, and the knee angle for a lower-limb power-assist robot. Pattern recognition and machine learning models using sEMG signals have several inherent problems for gait sub-phase detection. These problems are due to recognition delay, lack of consideration for the unique characteristics of sEMG signals based on the subject, and meaningless features. To solve these problems, we propose a new labeling technique based on the heel and toe, a muscle and feature selection, a user-adaptive classifier using a weighted voting technique to achieve gait sub-phase detection, and a gait sub-phase prediction technique using interpolation. Experimental results show that the average accuracies of the proposed labeling, the muscle and feature selection, and the user-adaptive classifier using weighted voting are 7%, 12%, and 17% better, respectively, than the existing methods using physical sensors. Results also show that the average prediction time of the proposed method is 80% faster than the existing methods.

1. Introduction

Owing to advances in information technology and biotechnology, studies have been conducted on bionic legs, smart walkers, powered orthoses, lower-limb power-assist robots, forearm discrimination, locomotion mode, and gait cycle detection [1–9]. A common goal of these studies is to achieve high motion-detection accuracy and a low time delay. The lower-limb human motion-detection system uses a foot switch, pressure sensor, an inertial measurement unit (IMU) sensor, and the surface electromyogram (sEMG). The IMU is the most widely used method for detecting human lower limb movements, because it can easily acquire the knee angle, which is the core of motion recognition. However, the IMU is sensitive to environmental changes, such as surface conditions, and detailed gait analysis is difficult. Therefore, various studies using the sEMG signal as an auxiliary signal are under way. Muscle activity analysis using sEMG signals permits the detection of complex human motion more accurately than other sensors [4–6].

Therefore, we implement a system in which the main signal uses the sEMG, and the auxiliary signal uses the IMU to increase the motion detection accuracy and reduce the time delay. However, the gait sub-phase detection system using the sEMG as the main signal causes a lot of problems in detection. If the sEMG signal is used to detect the gait sub-phase using a real-time pattern recognition model for the lower-limb power-assist robot, four issues arise. First, performing sEMG signal-based pattern recognition to detect gait sub-steps can yield results at the middle or end of the action, but latency issues can occur [7,8]. Second, multiprocessing computing overhead issues can occur when processing multi-channel sEMG stream data. That is because multi-dimensional operations and classifiers are required when performing pattern recognition using multi-channel sEMG signals [12,13]. Third, when a surface-type EMG electrode is used, the period and the muscle activity of the individual gait sub-phase may change depending on the subject's gait habit, skin type, body fat, and physical size [14–18]. Finally, gait sub-phase detection using pattern recognition and machine learning models may generate meaningless features, which reduces detection accuracy of the gait sub-phase.

In this paper, we propose a new gait analysis and detection system using sEMG signals. We also try to solve problems by composing two parts: *detection* and *prediction*. Detection solves the problem of classifying the walking cycle according to the user's walking method. Prediction assists in walking by predicting the next walking pattern of the user through the learned walking cycle and walking classification. In order to support these detection and prediction functions, we propose a new labeling technique based on the heel and toe, a muscle and feature selection technique, gait sub-phase detection using a weighted voting technique, and a

* Corresponding author.
E-mail addresses: kasame123@hotmail.com (J. Ryu), bhlee@sammicomputer.co.kr (B.-H. Lee), mjh91@iesl.inha.ac.kr (J. Maeng), deokhwan@inha.ac.kr (D.-H. Kim).

https://doi.org/10.1016/j.medengphy.2019.05.006
1350-4533/

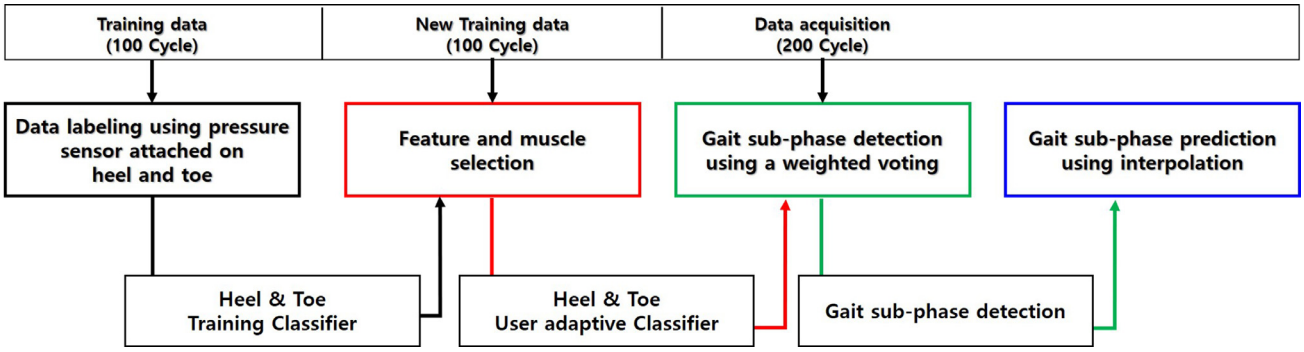

Fig. 1. Block diagram overview.

sub-phase prediction technique using interpolation of the gait sub-phase.

Fig. 1 shows a block diagram of the proposed algorithm. Gait sub-phase prediction and detection using sEMG signals for lower-limb power-assist robots consist of a training stage for learning the classifier, a training stage for muscle and feature selection, and gait sub-phase detection and prediction stages, sequentially.

Gait sub-phase labeling based on the heel and toe is divided into four gait sub-phases (initial contact, mid-stance, propulsion, and swing) according to the results of the heel classifier and the toe classifier. The heel and toe classifiers are used to determine whether the heel and/or toe are touching the ground. This method helps to extract meaningful feature values, because this algorithm uses the muscle activity detected when the heels and/or toes touch or leave the ground.

Muscle and feature selection generate a user-adaptive classifier by selecting muscles and features with high gait sub-phase detection accuracy for each subject. To do this, a threshold is chosen empirically to determine the best combination of feature set and classifier group. Finally, we achieve gait sub-phase detection using weighted voting and prediction using interpolation. This method reduces classification overhead by using a binary classifier, and improves gait sub-phase detection accuracy. This is because it only uses muscles and feature values showing high detection accuracy for each subject, and it uses a one-dimensional classifier. It also recognizes the gait sub-phase using the weight of each feature value.

The gait sub-phase prediction technique using interpolation predicts the next period of the gait sub-phase using its past period. Pattern recognition and machine learning models take at least 300 ms to collect EMG signals for human motion recognition. However, the period of the average human gait cycle is about 1300 ms, and that of a minimum-gait sub-phase (initial contact) is less than about 130 ms. To solve this problem, period prediction for the gait sub-phase is necessary in order to control a lower-limb power-assist robot using EMG signals.

2. Method

2.1. Data acquisition

The subjects provided written informed consent prior to the experimental procedures, which were performed in accordance with the Declaration of Helsinki and approved by the Inha University Institutional Review Board (approval: 150603-1A). A commercial sEMG device (MP150, BIOPACK Systems, Inc.) for amplifying sEMG signals, six BioPac BN-EMG2 units with 12 channels, and BioPac EL503 units (i.e., pre-gelled disposable electrodes) were used. The sEMG signal acquisition device acquired the raw data using a 20–450 Hz band pass filter, a 1 kHz sampling rate, and 16-bit analog-to-digital converter.

Fig. 2(a) shows a subject's level-walking scene and the electrode mounting position. For data acquisition, nine sEMG channels were attached to the sartorius (SART), rectus femoris (RF), vastus medialis (VM), vastus lateralis (VL), tibialis anterior (TA), semitendinosus (ST), biceps femoris (BF), peroneus longus (PL), and gastrocnemius (MG) muscles. All electrodes were placed in pairs at a separation distance of 1.5–2 cm according the guidelines of the sEMG for non-invasive assessment of muscles (SENIAM) and the International Society of Electrophysiology and Kinesiology (ISEK).

In general, the walking phase is classified into 8–11 stages based on the knee angle and according to the sensor used in the experiment. For this purpose, many sensors, such as infrared ray, markerless, pressure, IMU, and Force/Torque, are used making it difficult to produce light aids. In this paper, we shortened walking to four steps for detection and prediction using only the sEMG, the IMU, and the pressure sensor.

We produced a physical sensor data acquisition board in order to label the gait sub-phase in the training stage. The micro controller unit (MCU) of the physical sensor data acquisition board used the STMicroelectronics STM32F4DISCOVERY, with a width of 32 cm, a height of 60 cm, and weight of 640 g. The board was equipped with two pressure sensors to check whether the heel and toe were touching the ground, and an attitude/heading reference system (AHRS) sensor to check the knee angle. In addition, the AHRS sensor was used as auxiliary data to distinguish between stance and swing by changing the angle. An sEMG signal and physical sensor data acquisition program (AcqKnowledge 4, BioPac Systems) was used. To collect the sEMG signal and sensor data, each subject performed 400–500 walking steps.

2.2. First training stage using labeling based on heel and toe

As shown in Fig. 3, two training datasets representing heel and toe states were generated from identical sEMG signals, IMU and two pressure sensor data. Feature value sets were extracted from two categories of training data based on these states. The heel and toe classifiers can yield four gait sub-phases by separating the heel state (touching the ground or not) and the toe state (touching the ground or not). The state of touching the ground represents neuromuscular activity, while not touching the ground represents neuromuscular inactivity of the muscles associated with walking; it is therefore possible to extract meaningful feature values.

The first training stage using pressure and AHRS sensors attached to the heel and toe consists of three steps. In the first step, the training dataset (100 gait cycle data recordings) is labeled using a physical sensor board. The input dataset is labeled with a two-digit binary number that indicates whether the heel

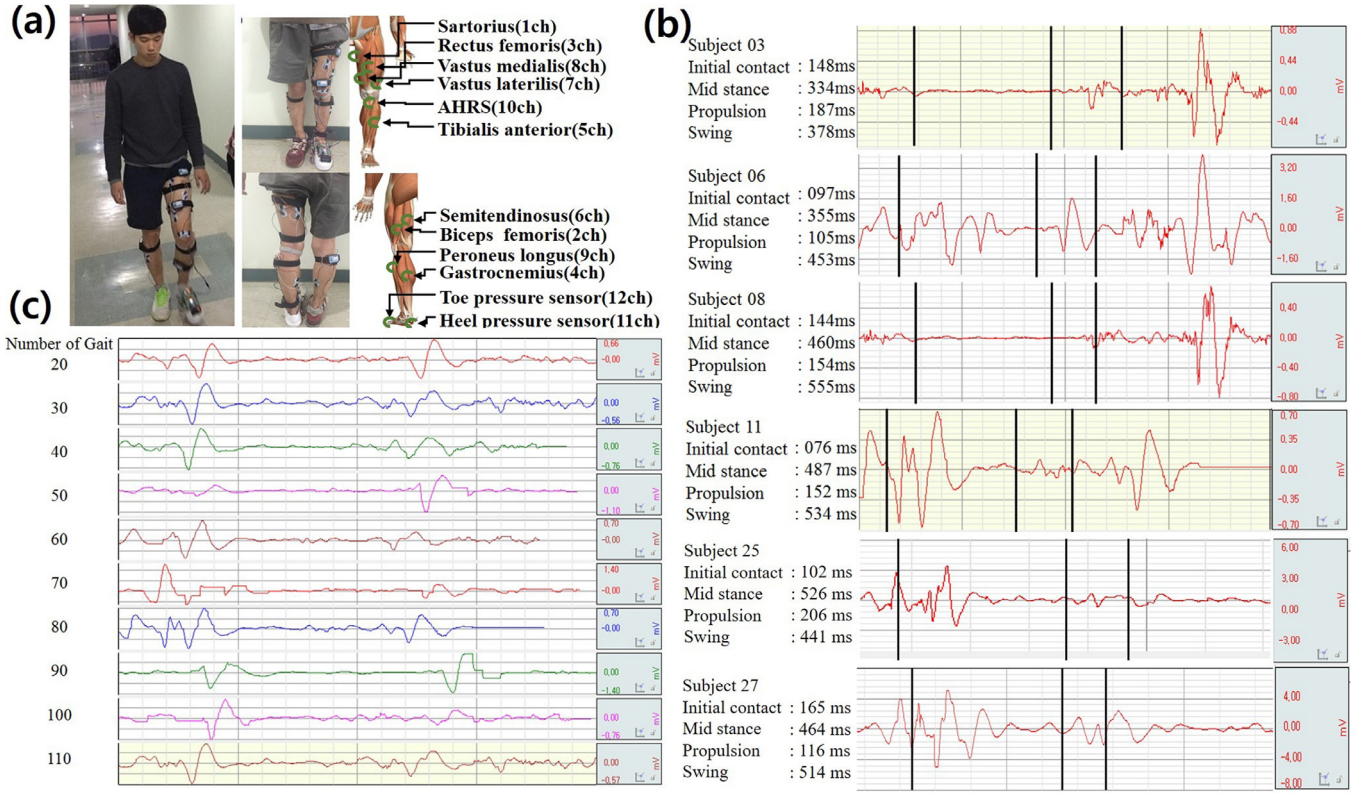

Fig. 2. Pictures of experimental procedures and acquired signals: (a) a subject's level-walking scene and electrode mounting position, (b) average sEMG signals extracted from the sartorius muscle, and (c) sEMG signals of subject 3 corresponding to gait cycle number.

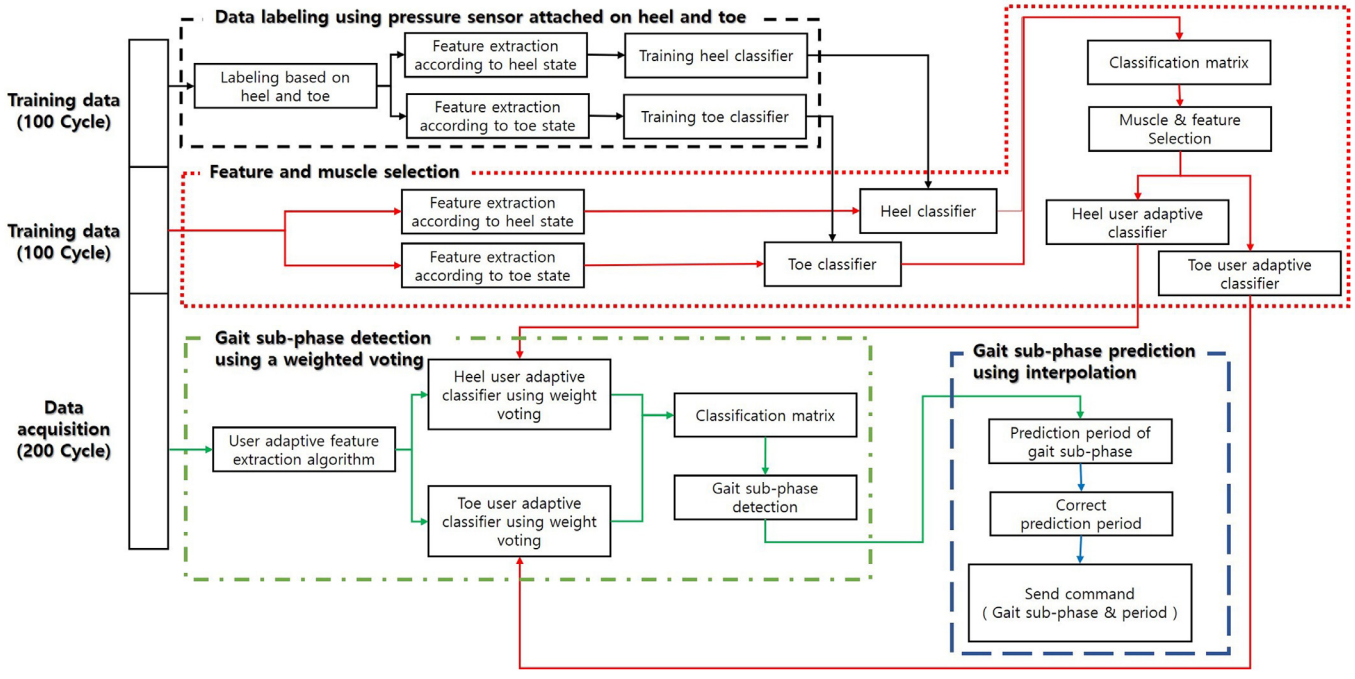

Fig. 3. Block diagram of gait sub-phase detection and prediction using a user-adaptive classifier.

and toe touch the ground. In the second step, 12 feature extraction algorithms are applied to the labeled input dataset to extract feature values. Finally, the classifier groups (heel classifier and toe classifier) are learned using the linear discriminant analysis (LDA), quadratic discriminant analysis (QDA), and k-nearest neighbors (K-NN) machine learning methods based on the muscle channels and feature values [22]. Depending on the muscles and feature extraction algorithms applied at this stage, classifier groups were generated for all cases.

2.3. Second training stage using feature and muscle selection

The second training stage using muscle and feature selection consists of four steps. In the first step, another training dataset

(100 gait cycle data recordings) is labeled using a physical sensor board in order to evaluate the above classifier groups. In the second step, feature values are extracted, and the feature values from the new walking data are entered into the classifier groups generated in the training stage. In the third step, the gait sub-phases are detected using a classification matrix according to the classifier group, and the detection accuracy of all classifier groups was calculated by comparing the new walking labeling data and the results of the classifier groups. The gait sub-phase was classified into four phases in combination with the classification matrix, the results of the heel classifier, and the results of the toe classifier. Finally, the muscle and feature values corresponding to each gait sub-phase were selected. Feature and muscle selection uses classifier groups with calculated accuracies of more than 60% in the third step. This is done to select meaningful muscle and feature values by using classifier groups with high detection accuracy. In this study, the threshold values set of 60% for gait sub-phase detection showed the highest detection accuracy (see Section 3.3). In the gait sub-phase detection stage, we detected the gait sub-phase using only the selected muscle and feature values at this stage. At this time, the calculated accuracies of classifier groups were used as parameters for weighted voting at the gait sub-phase detection stage.

2.4. Gait sub-phase detection stage using a weighted voting technique

The gait sub-phase detection stage consists of three steps. In these steps, gait initiation during initial contact is recognized using the VL and VM muscles [19]. In the first step, feature values are extracted using selected feature extraction algorithms and are entered into the selected classifier groups in the training stage using muscle and feature selection. The second step involves detection of the heel state and toe state using a weighted voting technique. The weighted voting technique consists of four steps. In the first step, the weight of each muscle and toe classifier or heel classifier is calculated according to the feature values. The feature values were weighted using the following equation:

$$WF_k = F_i \times \ (F_i - 60) \Big/ \sum_{i=1}^{n} (F_i - 60) \tag{1}$$

where F_i is the accuracy of the ith feature extraction algorithm, $k = 1,2,3, \ldots, f$ (in which f is the number of selected features), n is the total number of feature extraction algorithms according to muscle, and 60 is the threshold value determined through the experiments described in Section 3.3. Eq. (1) calculates weights using the detection accuracy of each feature value obtained in the training stage using muscle and feature selection [20]. The numerator of the weighted average is the product of the accuracy value and –60 (the threshold value; see Section 3.3). In the second step, the detection results for muscles using the feature value weights were selected. The muscle results were calculated using the following equation:

$$WM_{j,ON} = \sum_{k \in \gamma_{j,ON}} WF_k$$

$$WM_{j,OFF} = \sum_{k \in \gamma_{j,OFF}} WF_k$$

$$Voting\ results\ at\ j\text{th}\ muscle = \begin{cases} ON, \ WM_{j,on} > WM_{j,off} \\ OFF, \ otherwise \end{cases} \tag{2}$$

where *Sum of the* WF_k is the sum of weighted kth selected muscle, $k = 1,2,3, \ldots, m$ (in which m is the number of selected muscles), $\gamma_{j,ON}$ is the number of selected feature extraction algorithms from the jth selected muscle where the result of the classifier is "on"; $\gamma_{j,OFF}$ is the number of selected feature extraction algorithms from the jth selected muscle where the result of the classifier is "off"; $WM_{j,ON}$ is the sum of the WF for the jth selected muscles for recognition where the result is "on"; and $WM_{j,OFF}$ is the sum of the WF for the jth selected muscles where the result is "off." In the fourth step, the muscle weights are used to obtain classifier detection results, calculated using the following equation:

$$MS_{ON} = \sum_{j \in \beta_{ON}} WM_{j,s}$$

$$MS_{OFF} = \sum_{j \in \beta_{OFF}} WM_{j,s}$$

$$Voting\ Result = \begin{cases} ON, \ MS_{on} > MS_{off} \\ OFF, \ otherwise \end{cases} \tag{3}$$

where s denotes the classification results at the jth muscle, β_{ON} is the number of selected muscles for which the result of the classifier is "on"; and β_{OFF} is the number of selected muscles for which the result of the classifier is "off." That is, it selects the class that acquires the highest weight as the result.

In the third and final step in the gait sub-phase detection stage, using the classification matrix, the results of the heel classifier and the toe classifier determine the gait sub-phase of the input window of the current period using the classification matrix by combining the results of the heel and toe classifiers.

2.5. Prediction stage using new gait sub-phase prediction using linear interpolation

We propose a gait sub-phase prediction technique using interpolation. This technique uses interpolation to predict the period of the gait sub-phase in the next gait cycle using the period in the preceding gait cycle and the period in the current gait cycle. In addition, it can correct the prediction period using the change in the period of the current gait cycle in order to minimize the difference between the real and predicted periods when performing gait sub-phase prediction. For example, we assume that the initial contact was detected. First, the period of the initial contact in the next gait cycle is predicted using the period of the current gait sub-phase, the period of initial contact in the previous gait cycle, and the period of initial contact in the gait cycle before the previous gait cycle. Finally, the predicted period of initial contact is corrected by using the difference between recognition and prediction periods of the propulsion, the mid-stance, and the initial stance in the current gait cycle, and of initial contact in the previous gait cycle when the propulsion is in the current gait sub-phase.

The gait sub-phase prediction technique using interpolation consists of two steps. Fig. 5 shows an example of gait sub-phase prediction using linear interpolation. In the first step, the predicted period of the gait sub-phase in the next gait cycle and the correction value are calculated. The predicted period and correction values are calculated using the following equation:

$$p_{i+1,j} = T_j + \frac{e + c}{2}$$

$$e = \frac{\sum_{n=0}^{2} \left\{ g_{i-n,j} - g_{i-n-1,j} \right\}}{3}$$

$$c = \frac{\sum_{n=0}^{GP-1} \left\{ g_{i,j-n} - p_{i,j-n} \right\}}{GP} \tag{4}$$

where i is the current gait cycle, and j is the current gait sub-phase. That is, j values of 1, 2, 3, and 4 denote initial contact, mid-stance, propulsion, and swing, respectively; $g_{i,j}$ is the recognized period of the ith gait cycle and the jth gait sub-phase, and $p_{i+1,j}$ is the predicted period of the $i+1$th gait cycle and the jth gait sub-phase. T_j is the average period of the ith gait sub-phase

calculated in the training stage, and *GP* is the number of total gait sub-phases; *e* is the average difference period of the *j*th gait sub-phase from the current gait cycle to the gait cycle two steps previously, and *c* is the average difference period of the current gait cycle calculated using the recognition period and the prediction period. Moreover, $p_{i+1,\ j}$ is the product of T_j and the average of *e* and *c*. In the second step, the prediction period of the *i*th gait cycle of the $j+2$th gait sub-phase is corrected by *c*, and the period of the $j+2$th gait sub-phase is passed to the robot. The prediction period of the $j+2$th gait sub-phase calculated in the previous gait cycle is corrected in order to reflect the period changes in the current gait cycle before transmission to the robot. In other words, if the current gait sub-phase is that of initial contact, the prediction period of current propulsion calculated in the previous gait is corrected using *c*. The correct prediction period passed to the robot is calculated using the following equation:

$$p'_{i,j+2} = p_{i,j+2} + c \tag{5}$$

where $p_{i,j+2}$ is the prediction period for the *i*th gait cycle and the $j+2$th gait sub-phase calculated in the previous gait cycle. The correct prediction period $p'_{i,j+2}$ is calculated by adding correction value *c* and prediction period $p_{i,j+2}$. The correct prediction period, $p'_{i,j+2}$, is transmitted to the robot in the current or next gait sub-phase, and the robot is operated after next gait sub-phase according to $p'_{i,j+2}$.

3. Results and discussion

Twenty-seven subjects (14 males and 13 females, including three elderly males) with an average age of 24 years old (±1.8 standard deviation [SD]) took part in this experiment. The age of the elderly subjects averaged 57.5 years old; their average height was 175 cm, average weight was 68 kg, and walking times ranged from 1.12 to 1.32 s with a mean of 1.27 s. The signals for two of the elderly subjects are shown as Subject 25 and Subject 27 in Fig. 1(b). The average age of the other subjects was 20–28 years old, and their heights ranged from 152 to 183 cm (± 7.3 SD), mean 168.8 cm, weight range 42–95 kg (± 10.9 SD), mean weight 61.9 kg, body weight index ranged from 17.5 to 30.7 (± 21.6 SD) with an average of 21.6, and their walking times ranged from 0.87 to 1.34 s (± 2.6 SD) with a mean of 1.13 s. All subjects had no history of lower extremity or other musculoskeletal disorders. Although there is a difference in waveform depending on the walking habits of a pedestrian, regardless of age, the proposed method is not different from that for general subjects because it is learned by each pedestrian.

Table 1 shows the information for age, weight, height, and BMI for male and female subjects. In total, 400 gait cycle data recordings were used in this experiment; 100 were used for the training stage using labeling based on the heel and toe, and another 100 were used for the training stage using muscle and feature selection. The remaining 200 were used as test data in the experiment, with the experimental program implemented in Matlab 2015.

Table 1
Information on age, weight, height, and BMI obtained from subjects.

Sex	Variables	Max	Min	Average	SD
Male	Age (years)	28	22	24.3	1.3
	Height (cm)	183	164	174.4	4.8
	Weight (kg)	95	53	67.8	10.7
	BMI (kg/m^2)	30.7	18.5	22.2	3.04
Female	Age (years)	26	20	24	2.18
	Height (cm)	168	152	163.5	5.0
	Weight (kg)	70	42	56.3	7.8
	BMI (kg/m^2)	24.8	17.5	21.0	2.3

We evaluated the average detection accuracy at the gait-phase detection stage (Section 3.3) and focused on reduction of the prediction time latency to evaluate it as technology suitable for real-time robots, since the accuracy of gait detection was already known at the gait sub-phase prediction stage (Section 3.4). Therefore, Section 3.4 uses the results of Section 3.3 to measure the prediction time.

3.1. Effect of subjects' characteristics

Fig. 2(b) shows the average sEMG signal pattern for the SART muscle with respect to subjects 3, 6, 8, and 11. Subjects 3 and 8 were confirmed to show sEMG signal activity corresponding to a normal gait cycle from initial contact to the swing stage, whereas sEMG signals of the other subjects showed similar patterns during only the stance stage. This is because the sEMG signal patterns of subjects measured at the lower-limb muscles varied, depending on the subject's gait habit, body fat, and skin type [10–13]. In contrast, the results show that the sEMG signals of the same subjects are similar and consistent with respect to various gait cycles. Fig. 2(c) shows the sEMG signal pattern of Subject 3 with respect to various gait cycles; despite a different gait, the sEMG signal pattern is similar. Therefore, we can see that the classifier for gait sub-phase detection should be learned from walking data of the same subject.

3.2. Effect of the threshold value on muscle and feature selection

We evaluated the accuracies of the proposed method corresponding to the threshold value in the training stage using muscle and feature selection. Fig. 4 shows the average detection accuracies and numbers of selected muscles according to the threshold value. The average accuracy and the number of selected muscles of the heel classifier according to threshold values between 60% and 75% were 93% (± 3.2 SD) and 3.7. In contrast, those of the heel classifier

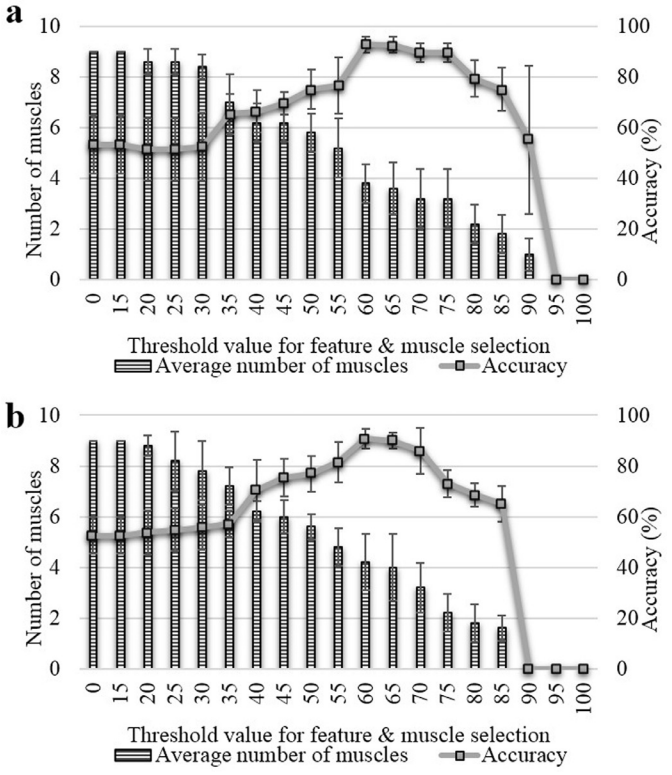

Fig. 4. The average accuracy and the number of selected muscles of the proposed method according to the threshold value: (a) heel classifier, (b) toe classifier.

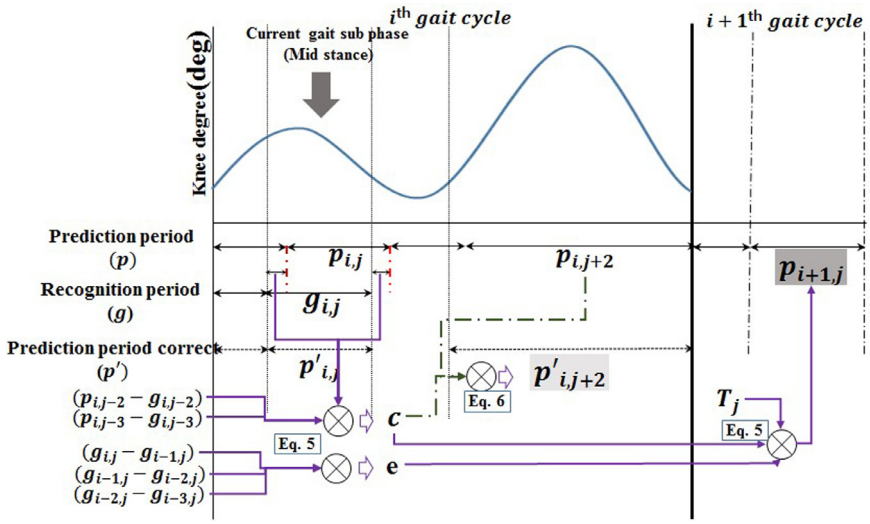

Fig. 5. Examples of gait sub-phase prediction using linear interpolation.

Table 2
Average sensitivity, specificity, and precision of the proposed method and the existing method according to classifier.

	Sensor	Features	Method	Sensitivity	Specificity	Precision	Accuracy
Proposed method	sEMG+IMU+PR	Selected muscles and features	LDA	96 (± 3.3 SD)	98 (± 3.2 SD)	97 (± 2.3 SD)	97 (± 2.2 SD)
			QDA	98 (± 1.1 SD)	98 (± 1.4 SD)	97 (± 3.7 SD)	98 (± 2.0 SD)
			kNN	98 (± 2.0 SD)	98 (± 3.7 SD)	99 (± 2.4 SD)	98 (± 2.1 SD)
Existing method (a)	sEMG+IMU+PR	All muscles and features	LDA	66 (± 8.4 SD)	85 (± 5.2 SD)	83 (± 4.2 SD)	77 (± 5.6 SD)
			QDA	68 (± 8.3 SD)	84 (± 4.7 SD)	82 (± 4.6 SD)	81 (± 4.7 SD)
			kNN	68 (± 9.0 SD)	85 (± 4.3 SD)	82 (± 5.3 SD)	81 (± 4.8 SD)
Existing method (b)	IMUs	All muscles and features	kNN	87 (± 4.3 SD)	91 (± 4.1 SD)	93 (± 3.8 SD)	90 (± 3.7 SD)
	IMUs+PR		kNN	89 (± 3.7 SD)	92 (± 3.7 SD)	95 (± 3.2 SD)	93 (± 3.1 SD)
	PR		kNN	83 (± 8.0 SD)	88 (± 9.0 SD)	76 (± 7.0 SD)	79 (± 8.6 SD)

when threshold values were less than 55% or higher than 80% in the training stage using muscle and feature selection resulted in 77% (± 11 SD) and 5.2 (±1.2 SD), and 79% (± 7.1 SD) and 2.2 (± 0.7 SD). There was no significant difference in accuracy using a threshold value of 60% versus 75% (analysis of variance [ANOVA], $F = 1.03$, $P > 0.01$). However, accuracy at the threshold value of 60% was significantly different from that at the threshold values of 55% (ANOVA, $F = 11.8$, $P < 0.01$) and 80% (ANOVA, $F = 11.66$, $P < 0.01$).

The average accuracy values and numbers of selected muscles of the toe classifier using threshold values between 60% and 70% were 91% (± 5.1 SD). In contrast, the average accuracy and the number of selected muscles using threshold values less than 50% or higher than 75% from the training stage using muscle and feature selection results in 77% (± 7.0 SD) and 5.6 (± 0.5 SD), and 73% (± 5.4 SD) and 2.2 (± 0.7 SD), respectively. There was no significant difference in accuracy at threshold values of 55% to 70% (ANOVA, $F = 1.67$, $P > 0.01$). These results are noteworthy in the case of threshold values less than 60%, which generated meaningless feature values, because muscles not associated with the sEMG patterns of the gait sub-phase were used in the gait sub-phase detection stage. In addition, for threshold values more than 75%, this was reflected in the results without correcting the feature values generated by the error pattern, because selections included fewer than two muscles. Therefore, they have a lower average and a higher SD in accuracy. In contrast, for threshold values between 60% and 65%, accuracy was 87% better and had a lower SD than other threshold values, because the muscles of clear sEMG signal patterns and the muscles used to correct the error pattern of sEMG signals for specific muscles were selected. Therefore, we determined that the threshold of the training stage using muscle and feature selection should be 60%.

3.3. Performance evaluation of gait sub-phase detection

We evaluated the sensitivity, specificity, precision, and accuracy of the proposed method and the existing methods. To do this, as shown in Table 2, we categorized existing methods into two directions: existing method (a) using 12 features and EMG and physical sensors, and existing method (b) using the same 12 features but physical sensors only. The proposed method, however, uses a combination of selected features and EMG and physical sensors.

First, existing methods use 12 features, such as variance (VAR), Willison amplitude (wAMP) [21], zero crossing (ZC), root mean square (RMS) values, slope sign changes (SSC), mean absolute values (MAV), integrated EMG (iEMG), modified mean absolute value 1 (MMAV1), modified mean absolute value 2 (MMAV2), mean absolute value slope (MAVSLP), waveform length (WL), and simple square integrals (SSI), while the proposed method uses a combination of less than 12 features through the feature and muscle selection process. Second, in terms of sensor usage, existing method (a) and the proposed method use sEMG, IMU, and pressure(PR) sensors, whereas existing method (b) uses a physical sensor only. Existing method (b) includes existing method_IMUs [24] using IMU sensors, existing method_IMUs+PR sensors [25] using IMUs and PR sensors, and existing method_PR using pressure sensors. Branches were compared. See Table 2, existing method (b).

LDA, QDA, and kNN classifiers were used in the proposed method and existing method (a), while kNN was applied to existing method (b). Table 2 shows the average sensitivity, specificity, precision, and accuracy of the proposed and existing methods per gait sub-phase. The results were obtained as true–false positives–

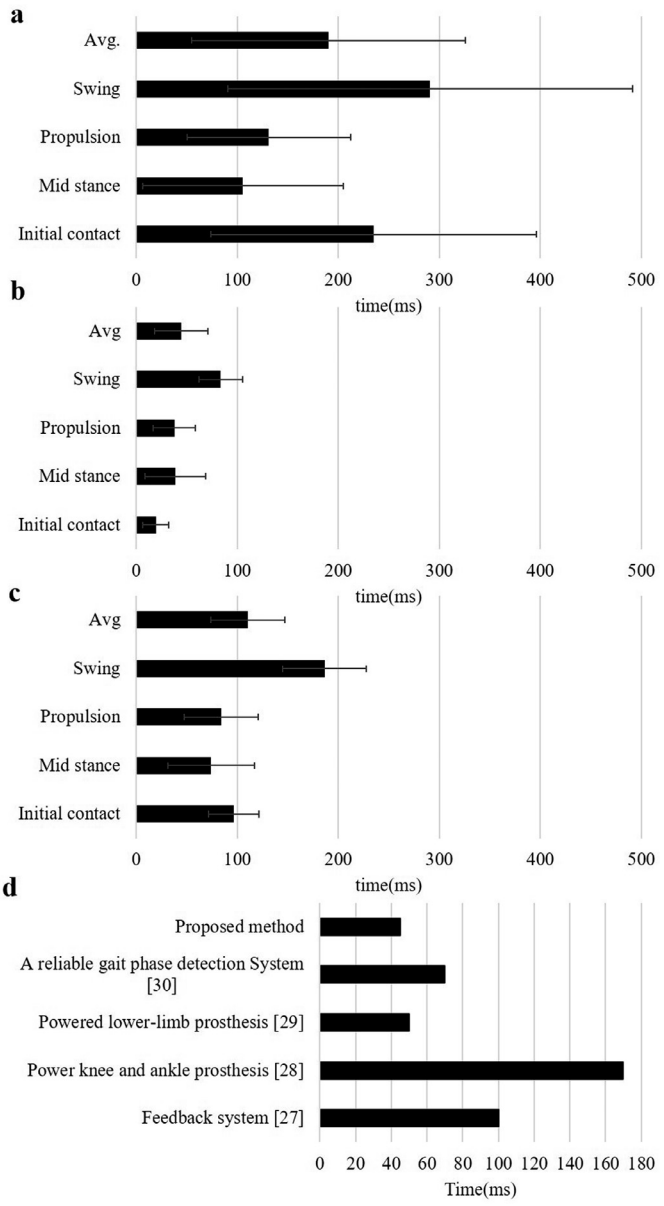

Fig. 6. Detection latency time: (a) existing methods, (b) proposed method, (c) proposed method without a prediction technique, and (d) performance of various lower-limb systems.

negatives of the gait sub-phase. Sensitivity represents the probability that the gait sub-phase is true positive for true positive (correctly identified) and false negative (incorrectly rejected), while specificity represents the probability of determining true negative (correctly rejected) and false positive (incorrectly identified) for true negative [23]. Precision is used to correctly classify a true positive gait sub-phase between the true positive and false positive gait sub-phases. In this experiment, if the initial contact of the walking sub-phase was classified as the initial contact, it was calculated as a true positive. If it was classified as a different walking sub-phase, it was counted as a false negative. If the actual gait sub-phase was not an initial contact, and if the classification was also classified as a different gait sub-phase, it was calculated as a true negative, and if it was classified as an initial contact, it was calculated as false positive. The results show that the average accuracies of the proposed method are higher than the existing methods in all cases. We can see that the proposed method can separate true and false datasets better than the existing methods. This is because the proposed method can reflect the gait characteristics and muscle activity of an individual subject. We can also see that the proposed method detects false alarms better than the existing methods. This is because the proposed labeling process effectively separates gait sub-phases using muscle activity when the heel and/or toe touched the ground or left the ground. In addition, the proposed muscle and feature selection process can reduce the number of false alarms by minimizing the use of muscles generating unclear sEMG signal patterns. The existing method_IMUs and the existing method_IMUs+PR showed high accuracy similar to the previous studies because they use the angle of the knee to recognize the gait sub-phase. However, existing method (b) caused confusion in perceptions of occasional irregular walking by the subject.

3.4. Performance evaluation of gait sub-phase prediction

We evaluated the latency in predicting the gait sub-phase for the proposed method and the existing methods. Fig. 6 shows the average latency when predicting the gait sub-phase using an existing method, in Fig. 6(a), using the proposed method, in Fig. 6(b), and using the proposed method without a prediction technique, in Fig. 6(c), for all participants.

The results show that latency with the proposed method was four times shorter than existing methods. This is because the existing methods incur longer detection latency due to overhead using multi-class classifiers and incorrect labeling in the training phase. Moreover, we ensure that the proposed method reduces latency to 80 ms or less. The prediction technique using linear interpolation makes our proposed method suitable for use in real-time robot control.

Lastly, Fig. 6(d) shows the real detection latency using physical sensors, and the calculated gait sub-phase prediction times using the proposed method. Fig. 6(d) shows an assessment of latency for the proposed method and various lower-limb robot systems [26–29]. We can see that the range of detection latency for the gait cycle or sub-phase was 50–170 ms. Therefore, the detection latency with the proposed method is similar to, or shorter than, existing robot systems.

4. Conclusion

In this paper, we proposed gait sub-phase detection using an EMG and an IMU with heel and toe labeling, muscle and feature selection, a user-adaptive classifier with weighted voting, and a gait sub-phase prediction technique to achieve gait sub-phase detection in real time. The contributions of the proposed method are as follows. Its heel- and toe-based labeling provides good class separation, and provides a user-adaptive classifier according to the subject's gait habit. Therefore, it can better reflect the gait characteristics of the subject, compared to existing methods. And it can reduce gait sub-phase detection latency. In future studies, we will apply the proposed method to lower-limb power-assist robots in real environments, and we will develop a sEMG signal-based human control interface for lower-limb power-assist robots.

Competing interests

None declared.

Acknowledgments

This work was supported by the Inha University Research Grant.

References

[1] Hargrove LJ, Simon AM, Young AJ, Lipschutz RD, Finucane SB, Smith DG, AKuiken T, et al. Robotic leg control with EMG decoding in an amputee with nerve transfers. J N Engl Med 2013;369:1237–42.

[2] Chen B, Zheng E, Fan X, Liang T, Wang Q, Wei K, Wang L. Locomotion mode classification using a wearable capacitive sensing system. IEEE Trans Neural Syst Rehabil Eng 2013;21:744–55.

[3] Kim DH, Cho CY, Ryu JH. Real-time locomotion mode recognition employing correlation feature analysis using EMG pattern. ETRI J 2014;36:99–105.

[4] Taborri J, Palermo E, Rossi S, Cappa P. Gait partitioning methods: a systematic review. Sensors 2016;16(1):66–86.

[5] Ryu JH, Kim DH. Real-time gait subphase detection using an EMG signal graph matching (ESGM) algorithm based on EMG signals. Expert Syst Appl 2017;85:357–65.

[6] Ryu JH, Lee LBH, Kim DH. sEMG signal-based lower limb human motion detection using a top and slope feature extraction algorithm. IEEE Signal Process Lett 2017;24:929–32.

[7] Mizuno H, Tsujiuchi N, Koizumi T. Forearm motion discrimination technique using real-time EMG signals. In: Proceedings of the 2011 annual international conference of the IEEE engineering in medicine and biology society, EMBC; 2011.

[8] Ryu JH, Kim SH, Lee MR, Kim DH. User adaptive classification based on sEMG and signal Gait phase prediction using linear interpolation. In: Proceedings of the RESKO academic symposium; 2014. p. 337–40.

[9] Winter DA. Biomechanics and motor control of human movement. John Wiley & Sons; 2009.

[10] Huang H, Zhang F, Hargrove LJ, Dou Z, Rogers DR, Englehart KB. Continuous locomotion-mode identification for prosthetic legs based on neuromuscular-mechanical fusion. IEEE Trans Biomed Eng 2011;58:2867–75.

[11] Ryu JH, Kim DH. Multiple gait phase recognition using boosted classifiers based on sEMG signal and classification matrix. In: Proceedings of the eighth international conference on ubiquitous information management and communication. ACM; 2014.

[12] Neumann DA. Kinesiology of the musculoskeletal system-E-book: foundations for rehabilitation. Elsevier Health Sci 2013.

[13] Du YC, Lin CH, Shyu LY, Chen T. Portable hand motion classifier for multi-channel surface electromyography recognition using grey relational analysis. Expert Syst Appl 2010;37:4283–91.

[14] Phinyomark A, Limsakul C, Phukpattaranont P. Application of wavelet analysis in EMG feature extraction for pattern classification. Measur Sci Rev 2011;11:45–52.

[15] Bovi G, Rabuffetti M, Mazzoleni P, Ferrarin M. A multiple-task gait analysis approach: kinematic, kinetic and EMG reference data for healthy young and adult subjects. Gait Posture 2011;33:6–13.

[16] MacLellan MJ, Ivanenko YP, Massaad F, Bruijn SM, Duysens J, Lacquaniti F. Muscle activation patterns are bilaterally linked during split-belt treadmill walking in humans. J Neurophysiol 2014;111:1541–52.

[17] Bartuzi P, Tokarski T, Roman-Liu D. The effect of the fatty tissue on EMG signal in young women. Acta Bioeng Biomech 2010;12:87–92.

[18] Sutherland DH. The evolution of clinical gait analysis part l: kinesiological EMG. Gait Posture 2001;14:61–70.

[19] Wentink EC, Schut VGH, Prinsen EC, Rietman JS, Veltink PH. Detection of the onset of gait initiation using kinematic sensors and EMG in transfemoral amputees. Gait Posture 2014;39:391–6.

[20] Lei H, Govindaraju V. A study on the consistency of features for on-line signature verification. Struct Syntact Stat Pattern Recognit 2004:444–51.

[21] Phinyomark A, Limsakul C, Phukpattaranont P. A novel feature extraction for robust EMG pattern recognition. J Comput 2009;1(1):71–80.

[22] Kim KS, Choi HH, Moon CS, Mun CW. Comparison of k-nearest neighbor, quadratic discriminant and linear discriminant analysis in classification of electromyogram signals based on the wrist-motion directions. Curr Appl Phys 2011;11:740–5.

[23] Fawcett T. An introduction to ROC analysis. Pattern Recognit Lett 2006;27:861–74.

[24] Kotiadis D, Hermens HJ, Veltink PH. Inertial gait phase detection for control of a drop foot stimulator: inertial sensing for gait phase detection. Med Eng Phys 2010;32:287–97.

[25] Chen B, Zheng E, Wang Q, Wang L. A new strategy for parameter optimization to improve phase-dependent locomotion mode recognition. Neurocomputing 2015;149:585–93.

[26] Varol HA, Goldfarb M. Real-time intent recognition for a powered knee and ankle transfemoral prosthesis. In: Proceedings of the IEEE tenth international conference on rehabilitation robotics. IEEE; 2007.

[27] Varol HA, Sup F, Goldfarb M. Multiclass real-time intent recognition of a powered lower limb prosthesis. IEEE Trans Biomed Eng 2010;57:542–51.

[28] Zhang F, Li P, Hou ZG, Lu Z, Chen Y, Li Q, Tan M. sEMG-based continuous estimation of joint angles of human legs by using BP neural network. Neurocomputing 2012;78:139–48.

[29] Pappas IP, Keller T, Mangold S, Popovic MR, Dietz V, Morari M. A reliable gyroscope-based gait-phase detection sensor embedded in a shoe insole. IEEE Sens J 2004;4:268–74.